A CONTINUING STUDY OF RF CONDITIONING AND RF VOLTAGE LIMITS OF THE FOUR-ROD RFQ CONFIGURATION

R.M. Hutcheon†, T. Tran Ngoc†, A. Schempp*, A. Gerhardt*
M. Kurz*, G. Bolme†† and S.O. Schriber††
Atomic Energy of Canada Limited, Research Company
Chalk River Nuclear Laboratories
Chalk River, Ontario, Canada K0J 1J0

Abstract

The use of the four-rod RFQ, particularly in high power, high duty factor applications, is being studied to determine its possible advantages over other RFQ configurations. Preliminary studies have suggested these include mechanical simplicity, lower cost and competitive rf efficiency. The present ongoing investigation is concerned with the adequacy of the thermal and mechanical design and with the rf conditioning and high voltage sparking limits of practical high average power four-rod structures. A high power test manifold and a two-module four-rod structure were designed, assembled and tuned at Chalk River. The unit was then shipped to Frankfurt for high power testing on the 200 kW, 108 MHz transmitter. The two module structure was operated in both pulsed and cw mode at voltages up to 1.8 and 1.0 x Kilpatrick respectively. The integrity of the demountable mechanical rf joint was established. New diagnostic procedures based on infra-red imaging and x-ray analysis were also tested.

Introduction

Several studies have explored the possible use of the 4-rod RFQ configuration as a simple, high power, high duty factor device for frequencies below 200 MHz[1-3]. However, some questions remain in the path to development of an engineered, practical and reliable high power four-rod RFQ.

The present collaboration is aimed at studying

1) the adequacy of a demountable garter spring rf joint at the structure base
2) the rf efficiency (shunt impedance) of the structure under high power cw operation
3) the thermal response of the structure
4) the rf conditioning and the sparking characteristics of the structure.

General Design Considerations for the Test Structures

The frequency to be used for the tests was determined by the available 108 MHz cw rf system at the University of Frankfurt. The bandwidth of this system is 0.5 MHz, so the structure frequency must be set accurately. The general design equations had already been established[2,3] and cold model measurements yielded single module dimensions shown schematically in Table I. The dual module structure, Fig. 1, approximates the basic building block unit one might use in a long multiple unit structure.

The mechanical design used OFHC copper throughout and all metal-to-metal joining of vacuum components was done by brazing with Cusil or silver solder. Previous studies have shown that when the modules are inserted in the vacuum tank (Fig. 2), the power dissipated in the tank walls should be only a few percent of that dissipated in the structure. Thus the tank walls were adequately water cooled by soft soldering several turns of coper tubing arund the tank exterior. A confirmation of how well the fields are confined to the structure is given by the fact that the resonant frequency of the dual module structure increased by only 1.0 MHz to 108.5 MHz when it was positioned in the tank.

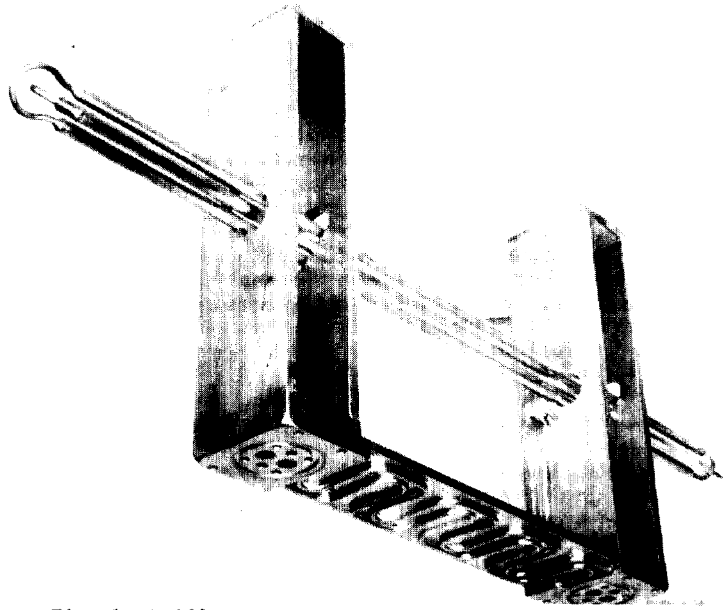

Fig. 1 A 108 MHz high power, dual module, 4-rod test RFQ, with unmodulated rods. Mounting the structure in the vacuum tank (Fig. 2) causes a +1 MHz frequency shift.

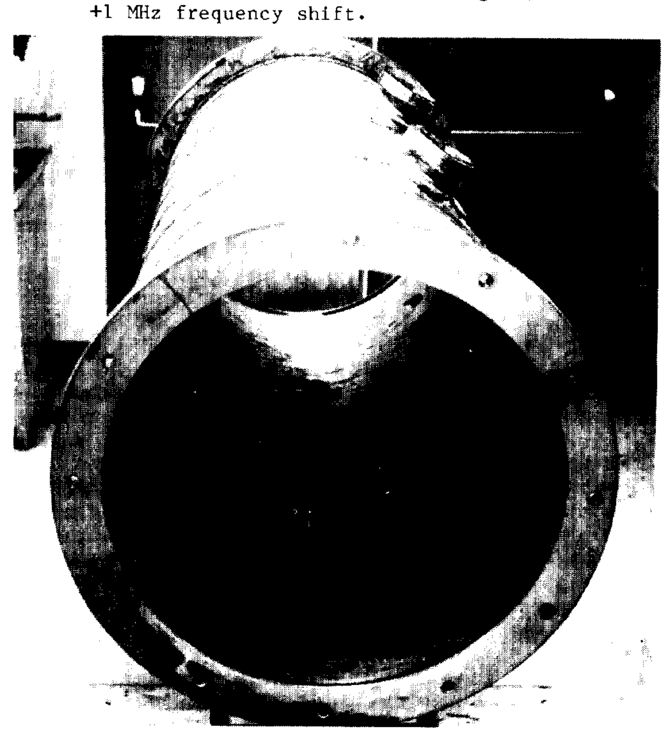

Fig. 2 Vacuum manifold for the 4-rod RFQ test structure. The two small protruding posts are where the demountable rf and vacuum joint is made with the inductor base plates.

* Universitat Frankfurt/Main, West Germany. Worked supported by BMFT.
† Work supported in part by DOE Contract No. 9-X5d-7843D-1.
†† Los Alamos National Laboratories, Los Alamos, New Mexico.

CH2387-9/87/0000-1794 $1.00 © IEEE

Another result of the concentration of the rf currents on the inside surfaces of the inductors is that the current flowing from the base of the inductor down the support post to the tank wall (Fig. 3) is small. Cold model measurements showed these surface current densities to be a few percent of those in the inductor interior. Experience suggested that the demountable joint shown in Fig. 3 should work in this location. The garter spring provides adequate rf contact and the "O-ring" at a larger radius provides the vacuum joint. The same principle is applied to the seal between the end flanges and the tank - again, because the currents are low. It should be noted that this type of joint would fail immediately if used as a demountable vane-base joint in a high power cw four-vane RFQ.

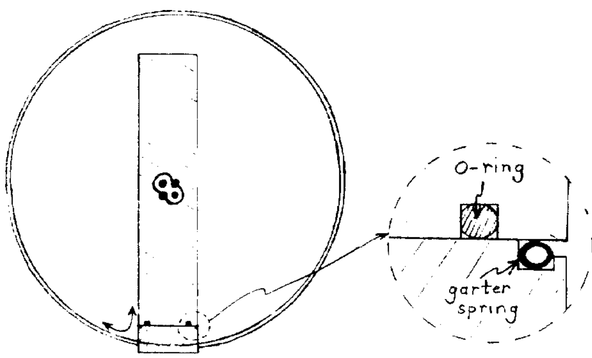

Fig. 3 A schematic cross-section of the structure mounted in the tank, showing details of the demountable rf and vacuum joint. Such a joint is possible because the inductor-to-vacuum tank currents are only a few percent of the interior inductor currents.

The Dual Module Structure - A High Power Test of the Concept

Construction and Tuning

The unit dimensions for the 108.5 MHz dual module structure were established with low power models (Table I), the total rod length being 0.94 m.

Table I

Unit Dimensions for the Dual Module Structure

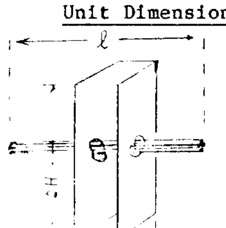

$2H = 400$ mm
$h = 62$ mm
$W = 110$ mm
$r_o = 9.15$ mm
$\rho = 6.35$ mm
$\ell = 470$ mm
$g = 9.2$ mm

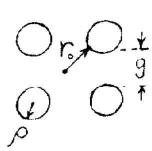

The theoretical Q, shunt impedance per unity length Z, and R_p value for such a structure, made of pure copper, were derived using the equations in reference 2 using y = 0.2. Note that the R_p value is defined by $R_p = V_p^2/2P$ where P is the dissipated power and V_p the peak rod-to-rod voltage.

$$Q_{TH} = 9156$$
$$Z_{TH} = 0.37\ \text{M}\Omega\text{-m}$$
$$R_p^{TH} = 0.20\ \text{M}\Omega$$

The measured Q value was 5400, which would predict a shunt impedance of Z = 0.22 MΩ-m.

At 100 kW power, this would give a peak voltage of 153 kV which, with V_p/g = 16/6 MV/m and a gradient enhancement factor of x 1.23, is equivalent to 1.75 Kp.

Operation and Test Results

After construction, tuning and cold testing at Chalk River, the tank and dual module were shipped to Frankfurt where the unit was installed in a lead-lined room, critically coupled to the rf system and evacuated with a 350 L/s pumping system. After low power runs at a few kW cw, the system was brought to a base pressure of $1.3 * 10^{-4}$ Pa ($1 * 10^{-6}$ Torr). Following this, the structure was gently conditioned, first with short pulses of increasing peak power and then with alternating low power cw and increasing duty factor long pulse mode (Table II) interspersed with long pumping periods.

During the last five hours of this conditioning period an AGEMA 870 infra-red imaging system with a 7° lens was used to observe the structure surface temperatures in the region where the rods attach to and pass through the inductor plates (Fig. 4). "Canon" extender tubes were used to reduce the focal length to 0.8 metres, and the field of view to ≈ 70 x 70 mm.

Unfortunately the sapphire window used for the IR viewing had a restricted aperture (≈ 35 mm) and, except during an initial high temperature cw run, affected the absolute temperature calibration. Although an attempt has been made to correct for this, absolute temperature values should be considered only approximate (Table III). Relative values should remain quite good.

Table II

Initial High Power Conditioning Runs

Run Time (h)	Peak Power Final (kW)	Duty Factor	Pulse Length (ms)	Pressure (10^{-4} Pa)	Frequency (MHz)
1	91	0.02	0.2	1.0	108.498
2	80	0.04	0.8	1.2	108.461
3.5	18	cw		0.65	108.335
3.5	61	0.10	5.0	0.5	108.437
2	30	cw		2.0	108.201
3.5	39	0.25	0.5 - 10	0.5	108.412

A few hot spots are clearly visible (Fig. 5) and it is tempting to associate them with the "glow points" often seen under similar conditions[4]. These spots are located at a point of high electric field - along the edge of the hole in the inductor plate through which the rods go (Fig. 4). The measured spot temperatures of ≈ 200°C may be seriously underestimated since the camera is averaging a pixel over ≈ 0.5 x 0.5 mm, and the spots could be much smaller than this. As expected, the warmest "non-spot" area is at the joint between the rod and inductor on the inside inductor surface, where the rf surface current densities are highest. The run at 25% duty factor with 0.5 to 10 ms pulse lengths showed no significant variation in the "hot spot" temperature, indicating that the spots reach their temperature or at least come to maximum energy dissipation in less than 0.5 ms.

Table III

Measured Surface Temperatures on the Inductor Central Region

Peak Power (kW)	Pulse Length (ms)	Maximum Temperature (°C) in Region (see Fig. 4) #1	#2	#3	#4
30	cw	65	68	208	114
38.7	0.5	46	49	103	95
38.7	1.0	47	46	93	63
38.7	1.5	49	49	104	69
38.7	2	49	47	100	67
38.7	3	48	48	99	66
38.7	4	48	47	90	64
38.7	5	47	47	103	68
38.7	10	47	46	95	63

One of the important questions to be answered is the actual shunt impedance of the structure. A computer based solid state x-ray energy analysis system was used to determine the end point energy of the bremsstrahlung spectrum of surface emission electrons crossing the rod-to-rod gap. After careful collimation and attenuation to reduce the count rate and pile-up effects, it was possible to obtain a reliable single photon spectrum from which to extract end points (Fig. 6). Several runs at 25% duty factor, 24 kW peak power and pulse lengths between 5 and 100 ms all yielded the same Rp value of 144 ± 4 kΩ. For the 0.94 m long structure, this means a shunt impedance of

$$Z_T^{meas.} = 0.27 \pm 0.01 \text{ M}\Omega\text{-m}.$$

This is within 25% of the simple theoretical estimate for the structure.

Summary

The collaboration is still in the early stages of testing the four-rod RFQ in a high power configuration. However, several conclusions can be drawn:

1) The shunt impedance of the structure is slightly higher than the simple theoretical estimates.
2) The demountable rf joint based on garter springs and "O"-rings was inspected and found in original condition after 90 kW pulsed and 30 kW-cw operation. There was no evidence of arcing at the joint.
3) The region of the hole in the inductor plates through which the rods go must be carefully designed for electrical stress reduction.
4) The water cooling system appears adequate although the flow rates may need to be increased for operation above 100 kW-cw.
5) The structure is amenable to easy transportation, is easily assembled and is fairly straightforward to condition, at least to 1 x Kp cw and 2 x Kp pulsed.

Future experiments will explore the structure under extreme high power and voltage conditions to test performance limits.

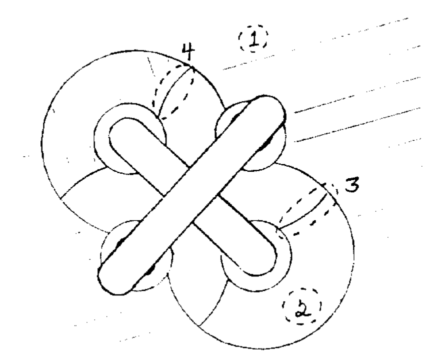

Fig. 4 End view of the inductor wall and the 4 rods. The numbered regions are respectively: 1 - the outside inductor surface (low rf currents); 2 - the interior surface of the inductor; 3 and 4 - areas along the edge of the inductor hole where hot spots occurred.

References

1. H. Klein et al., "Properties of a 0-Mode RFQ Structure and Recent Experimental Results", proc. 1981 Lin. Acc. Conf., LA-9234-C, 96 (1981).
2. R.M. Hutcheon, "A Modeling Study of the Four-Rod RFQ", Proc. 1984 Lin. Acc. Conf., GSI-84-11, 94 (1984).
3. G.E. McMichael, B.G. Chidley and R.M. Hutcheon, "Conceptual Design Study for the Proposed ISOL Post-Accelerator at TRIUMF", Atomic Energy of Canada Limited, Report AECL-8960 (1985).
4. R.M. Hutcheon et al., "Operation of a CW High Power RFQ Test Cavity: The CRNL "Sparker"", Proc. 1984 Lin. Acc. Çonf., GSI-84-11, 74 (1984).

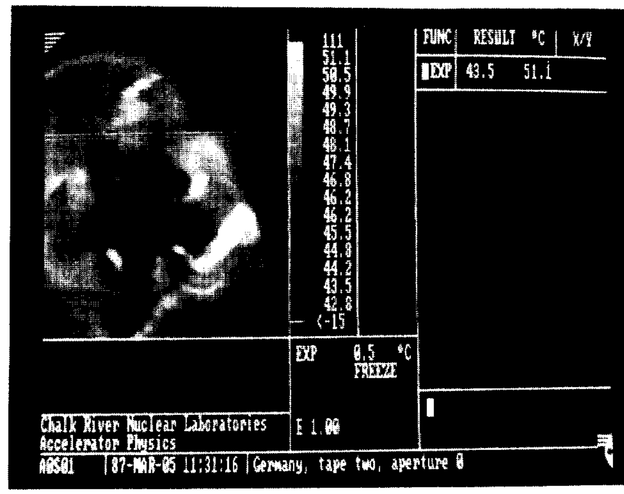

Fig. 5 A computer display of a typical measured temperature distribuiton. The regions may be identified, with some difficulty, by reference to Fig. 4.

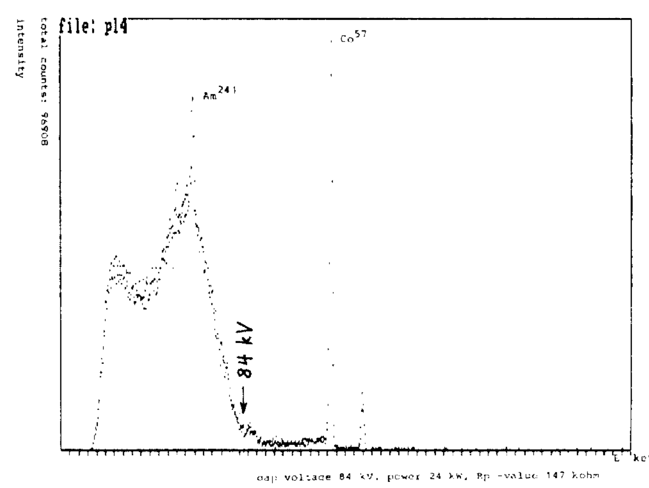

Fig. 6 A measured bremsstrahlung spectrum for operation at 24 kW, 100 ms pulse length and 25% duty factor. The estimated end point is 84 kV, yielding a R_p value of 147 kΩ. The gamma calibration lines are also shown.